2P5-10

Reconstruction of Tissue Scatterer Distribution from Ultrasound Echo Bayesian Inference

ベイズ推論に基づく超音波エコーからの生体組織散乱体分布の復元

Jing Zhu[1†], Atsumi Ubukata[1], Yihsin Ho[1], Norio Tagawa[1] ([1]Tokyo Metropolitan Univ.)
祝 婧[1†], 生方 暖美[1], 何 宜欣[1], 田川 憲男[1] ([1]首都大学東京)

1. Introduction

Ultrasonic scattering tends to occur when an ultrasonic wave propagates an object having a different acoustic impedance, which is sufficiently smaller than the wavelength. Scattering reduces the detectability of objects in ultrasound images, reduces contrast, and reduces the accuracy of ultrasound imaging. On the other hand, it should be noted that the ultrasonic imaging includes a signal obtained by a coherent summation of the echo signals from the scatterers within the tissue. Therefore, the tissue scatterer echo contains useful information, it should be kept.

As described above, since scatterers generate speckle patterns and hinder the detection of small objects, various suppression methods have been proposed. In recent years, study to reduce scatterer noise positively by capturing a small number of powerful echo sources is attracting increasing attention based on compression sensing and sparse modeling techniques. In this case, only the intensity of the echo is considered, and the characteristics of the scatterer are ignored. Based on these facts, in this study, we aim to recover the reflection distribution of the scatterers from echoes. When the small scatterers are correctly recovered, subtracting the corresponding echoes from the whole echo generates images consisting only of the strong and sparse scatterers, i.e., contours of organs, blood vessels, tumors, etc. In addition, by separately processing small scatterers and large reflectors, it is possible to image both separately. From the scatterer image, it may become possible to diagnose the tissue properties as a change from the time course and from the standard.

2. Method

Ultrasonic RF echo **y** is a synthesis of individual contributions from all scatterers placed randomly in a medium, and can be modeled as follows

$$\mathbf{y} = \mathbf{W}\mathbf{h} + \mathbf{n} \tag{1}$$

where **W** represents the convolution with the transmission pulse, **h** represents the equivalent reflectance, and **n** represents white Gaussian noise with a variance of σ_n^2.

As the transmission pulse becomes wide, the rank of **W** becomes close to zero. Thus, we can use $\mathbf{W}^+$ the pseudo-inverse of **W** to simply recover **h** as

$$\hat{\mathbf{h}} = \mathbf{W}^+\mathbf{y} \tag{2}$$

The solution is sensitive to the noise included in **y**, and the information contained in **h** and discarded by **W** cannot be recovered. Instead, we apply the AR model to **h**, and consider a method to recover discarded information by extrapolation [1].

Accordingly, the **h** of the scattered signals through an AR model is given by

$$h_i = \sum_{j=1}^{P} a_j h_{i-j} + \varepsilon_i \tag{3}$$

where $\mathbf{a} \equiv \{a_1, a_2, ..., a_P\}$ is called the AR parameter, P is the order of the AR model, and ε_i is white Gaussian noise with a variance of σ_h^2. In this case, **h** follows the multi-dimensional normal distribution, and its probabilistic density is

$$p(\mathbf{h} \mid \mathbf{a}, \sigma_h^2) = \frac{1}{\sqrt{(2\pi\sigma_h^2)^N \det\left(\mathbf{A}^t\mathbf{A}\right)^{-1}}} \exp\left(-\frac{1}{2\sigma_h^2}\mathbf{h}^t\mathbf{A}^t\mathbf{A}\mathbf{h}\right) \tag{4}$$

where, **A** is a matrix consisting of **a**. Then, according to Eq.1, the probabilistic density of **y** under the condition that **h** is given forms the following normal distribution.

$$p(\mathbf{y} \mid \mathbf{h}, \sigma_n^2) = \frac{1}{\sqrt{(2\pi\sigma_n^2)^N}} \exp\left[-\frac{(\mathbf{y}-\mathbf{W}\mathbf{h})^t(\mathbf{y}-\mathbf{W}\mathbf{h})}{2\sigma_n^2}\right] \tag{5}$$

Using Eqs.4 and 5, the joint probability is as follows:

$$p(\mathbf{y}, \mathbf{h} \mid \sigma_n^2, \sigma_h^2, \mathbf{a}) = \frac{1}{(2\pi)^N \sqrt{\sigma_n^{2N}\sigma_h^{2N} \det\left(\mathbf{A}^t\mathbf{A}\right)^{-1}}} \exp\left[-\frac{(\mathbf{y}-\mathbf{W}\mathbf{h})^t(\mathbf{y}-\mathbf{W}\mathbf{h})}{2\sigma_n^2} - \frac{\mathbf{h}^t\mathbf{A}^t\mathbf{A}\mathbf{h}}{2\sigma_h^2}\right] \tag{6}$$

In general, the parameters $\{\sigma_n^2, \sigma_h^2, \mathbf{a}\}$ are estimated as a maximum likelihood estimator (MLE) using the probabilistic density of **y** obtained by marginalizing Eq.6 with respect to **h**.

Finally, we can get the **h** determined as a maximum a posteriori (MAP) estimator $\hat{\mathbf{h}}_{MAP}$

$$\hat{\mathbf{h}}_{MAP} = \left(\frac{\mathbf{W}^t\mathbf{W}}{\sigma_n^2} + \frac{\mathbf{A}^t\mathbf{A}}{\sigma_h^2}\right)^{-1} \frac{\mathbf{W}^t\mathbf{y}}{\sigma_n^2} \tag{7}$$

In this way, the recovery using the AR parameters estimated based on the marginal likelihood is performed. The parameters in the AR model indicate the correlation intrinsic in the reflection distribution, and these are expected to

parameterize tissue properties. However, scatterers recovery must be treated as an ill-posed problem because the bandwidth of the signal is limited by characteristics of the transducer.

For the performance evaluation depending on the order of the AR model and the AR parameters, in this study, we set the order as 2 heuristically, so the AR parameters are the main evaluation parameter. Besides, since the observation noise is electric noise, we can suppose that σ_n^2 is known in advance.

3. Simulations

We confirmed the effectiveness of the proposed method through simulations using PZFlex, a standard FEM code for ultrasound analysis. An example of our simulated medium is given in **Fig. 1**(a). We assume that scatterers have random spatial distribution and the attenuation is homogeneous.

In the simulations, a linear array transducer with 128 elements was formed, each element width and each separation being 0.02 mm, respectively. In consideration of the size of scatterer, three different size scatterers were applied, and a 5 cycle pulse of 5 MHz shown in **Fig. 1**(b) was transmitted.

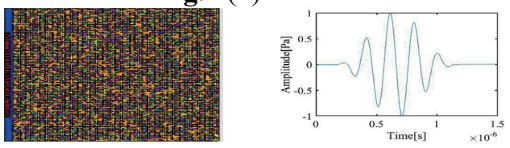

(a) (b)

Fig. 1 Simulation conditions: (a) example of simulation model; (b) transmitted signal;

4. Results and Discussion

As we can see that the different size scatterers are shown in **Fig. 2**. It can be easily seen that the size of scatterers increases in the order of (a), (b), and (c). **Figure 3** shows time series of a received echo signal, Through the **Fig.3**, we can vaguely distinguish the different sizes of the scatterers.

Figure 4 shows the result of recovered reflection distribution determined by the AR parameters. The estimated AR parameters in model (a) are a_1 =1.6326, a_2= -0.7019 and σ_h^2=0.133, in model (b) are a_1= -0.1759, a_2=0.7723 and σ_h^2=1.9871, while in model (c) there are a_1= -0.1513, a_2=0.8316 and σ_h^2=0.2913. As mentioned before, the noise variance σ_n^2 of the all models are set in 0.0009, when the peak amplitude of the transmission pulse was normalized, the standard deviation of noise was 3% of the standard deviation of **y**. It can be easily predicted from the recovered reflection distribution that the size of scatterers is different.

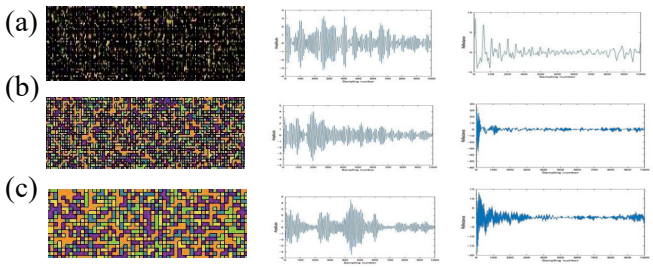

Fig.2 Different patterns of scatterers

Fig.3 Time series of echo signals

Fig. 4 Recovered reflection distributions

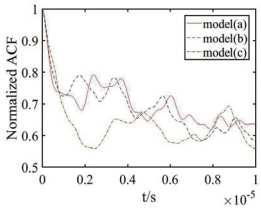

Fig.5 ACFs of echo signals

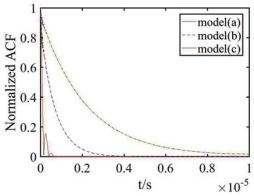

Fig.6 ACFs of recovered reflection distributions

As can be seen from **Fig. 5**, the red line, the black dashed line and the blue dash dot line are the auto correlation functions (ACFs) of the echo signals in model (a), model (b) and model (c), respectively. **Figure 6** shows the ACFs of the recovered reflection distributions in the same way. Even if the size of the scatterer increases, the ACFs of the echo signals does not seem to change much. However, the ACFs of the recovered reflection distributions change obviously. That is to say, we can evaluate the size of the scatterers by estimating the ACFs of the recovered reflection distributions.

5. Conclusion and Future Work

In this study, we present an estimation method of the scatterers distribution based on the Bayesian inference and the AR modeling from the echo. We analyze the relationship between the recovered reflection distributions and the AR parameters. The proposed method is confirmed to be effective for the observation of different scatterers compared to the echo signal and the recovered reflection distribution has better distinction. Furthermore, the ACFs of the recovered reflection distributions are expected to be applied to the quantitative analysis of scatterers.

Currently, the order of the AR model is set to 2, confirming other orders of the AR model will be a future task. Additionally, we are developing a new imaging system that separately display the boundary of the organ and the inside the organ.

References

[1] Atsumi Ubukata, et al, ICIEV 2017, Himeiji, Hyogo, Japan. Sep. 2017.